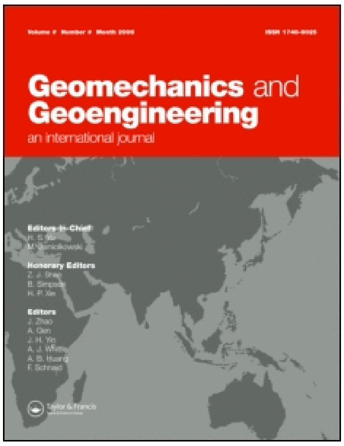

Geomechanics and Geoengineering
Publication details, including instructions for authors and subscription information:
http://www.informaworld.com/smpp/title~content=t725304177

Laboratory study of static and dynamic compaction grouting in triaxial condition

S. Y. Wang[a]; D. H. Chan[b]; K. C. Lam[c]; S. K. A. Au[d]
[a] Centre for Geotechnical and Materials Modelling, Department of Civil, Surveying and Environmental Engineering, The University of Newcastle, Callaghan, NSW, Australia [b] Department of Civil and Environmental Engineering, University of Alberta, Canada [c] Department of Building and Construction, City University of Hong Kong, Kowloon, Hong Kong [d] Department of Civil Engineering, The University of Hong Kong, Hong Kong

Online publication date: 13 February 2011

To cite this Article Wang, S. Y. , Chan, D. H. , Lam, K. C. and Au, S. K. A.(2011) 'Laboratory study of static and dynamic compaction grouting in triaxial condition', Geomechanics and Geoengineering, 6: 1, 9 — 19

To link to this Article: DOI: 10.1080/17486025.2010.521586

URL: http://dx.doi.org/10.1080/17486025.2010.521586

Geomechanics and Geoengineering: An International Journal
Vol. 6, No. 1, March 2011, 9–19

Taylor & Francis
Taylor & Francis Group

Laboratory study of static and dynamic compaction grouting in triaxial condition

S.Y. Wang[a]*, D.H. Chan[b], K.C. Lam[c] and S.K.A. Au[d]

[a]*Centre for Geotechnical and Materials Modelling, Department of Civil, Surveying and Environmental Engineering, The University of Newcastle, Callaghan, NSW 2308, Australia*; [b]*Department of Civil and Environmental Engineering, University of Alberta, Canada T6G 2W2*; [c]*Department of Building and Construction, City University of Hong Kong, Tat Chee Avenue, Kowloon, Hong Kong*; [d]*Department of Civil Engineering, The University of Hong Kong, Pokfulam Road, Hong Kong*

(Received 6 July 2009; final version received 1 September 2010)

This research paper is focused on the fundamental behaviour of applying static and dynamic compaction grouting techniques on completely decomposed granite (CDG) soils in Hong Kong. Using the modified triaxial apparatus and a novel pulse wave generator, laboratory tests were performed to identify the critical controllable factors of static and dynamic compaction grouting techniques in optimizing compaction effectiveness. The distinguishing feature of this laboratory apparatus is that it can simulate triaxial condition of static and dynamic compaction grouting. The effective confining pressure, the lateral pressure coefficient, excess pore water pressure, back pressure and void ratio change of the specimen were measured in this study. At the same time, the dynamic compaction grouting pressure, dynamic compaction frequency, and dynamic compaction duration were controlled. Moreover, the effects of effective confining pressure and injection rate on the compaction efficiency in static tests were studied. The study focused on the effect of dynamic compaction frequency, dynamic compaction duration, lateral pressure coefficient and initial dry density on the compaction efficiency of Hong Kong CDG soils.

Keywords: dynamic compaction grouting; injection rate; frequency; compaction efficiency

1. Introduction

The basic concept of compaction grouting technique to improve the mechanics properties of soils is injecting an expanding bulb of highly viscous grout with high internal friction into a compressible soil (Garf 1992, Warner 1992). This method has been extensively used to improve soil stiffness, reducing liquefaction potential, increasing bearing capacity of bored pile and compensating excessive ground loss due to underground construction. The compaction grouting procedure and its basic principle has been discussed by Garf (1969). The applicability of the proposed technique and experimental work including the case studies has been reported by Warner and Brown (1974). The application of compaction grouting to control ground movements due to tunneling was firstly introduced in the construction of the Bolton Hill Tunnel (Baker *et al.* 1983). Baker (1985) described the use of compaction grouting to compact liquefiable soils below dam embankments. Mair *et al.* (1994) reported the use of compaction grouting to limit settlement during tunneling. Boulanger and Hayden (1995) also reported the use of compaction grouting combined with dynamic compaction to densify deep, loose fill soils. Naudts and van Impe (2000) proposed a new compaction grouting technique for soil densification whereby the grout did not permeate or fracture the soil matrix. The key to this technique is installing a membrane/geotextile around the sleeves of the injection pipes to prevent leaking of grout into the surrounding soil.

Methods of using vibrating machines for soil compaction have also been developed. It results in a reduction of the volume of voids and requires rapid expulsion of fluids from the pore space. For example, vibro-compaction is a technique of improving the properties of granular soils by densification with a heavy vibrating probe which is inserted into the ground in conjunction with water jetting (Charles and Watts 2002). Vibro-compaction was first used in saturated natural fine sands, but it was soon applied to hydraulic fills (Jebe and Bartels 1983). Slocombe *et al.* (2000) reported that sands with higher fines content can be treated using new vibrators and modified construction techniques. In addition, dynamic compaction is a ground improvement technique by dropping a weight repeatedly on the ground surface. It is used to improve the bearing capacity of a wide range of materials (Mitchell and Jardine 2002). Greenwood and Kirsch (1984) described how tamping induces both punching shear and compaction displacement, as the momentum of the falling weight decays.

Dynamic compaction grouting is a new technique which combines traditional compaction grouting with vibro-compaction (Wang 2006). Owing to the characteristics

*Corresponding author. Email: Shanyong.Wang@newcastle.edu.au

ISSN 1748-6025 print/ISSN 1748-6033 online

DOI: 10.1080/17486025.2010.521586
http://www.informaworld.com

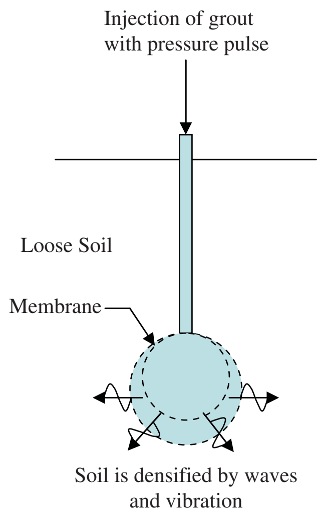

Figure 1. Schematic of dynamic compaction grouting.

of granular soil, such as sand, which is most effectively compacted using vibration, the new technique introduces vibrations to the membrane of a grouting bag during the expansion/compaction process (Figure 1). The grout is kept separated from the surrounding soil by a membrane, which means that the composition of the surrounding soil does not change during this process. The vibration of the membrane generates waves to the soil and moved the surrounding soil particles. Since the soil is in a loose state, movement of the soil particles results in a denser material.

There is no doubt that full-scale tests play an important role in evaluating the effects of grout composition, grouting pressure and injection rate on grout bulb development and soil response (Warner and Brown 1974). However, due to little control of site conditions and boundary conditions, questions remain unsolved regarding grout bulb development and soil response. Small-scale physical models provide valuable information for full-scale tests, or prototype events, if all important factors are correctly reproduced. Younis (1994), for example, conducted small-scale laboratory 1g-model compaction grouting tests to investigate grout bulb development and soil response. Au (2001), Soga *et al.* (2004) and Au *et al.* (2007) used modified consolidometer to study the compaction grouting effects by measuring the displacement of the top of the clay specimen under axi-symmetrical conditions.

This research focuses on the fundamental study of static and dynamic compaction grouting in completely decomposed granite soils (CDGS) of Hong Kong. For static tests, a series of compaction grouting tests were carried out to study the effect of the confining pressure and injection rates on the static compaction efficiency of CDGS. For the dynamic tests, more compaction grouting tests were carried out to study the effect of dynamic compaction frequency, dynamic compaction duration, the lateral pressure coefficient and initial dry density on the compaction efficiency of CDGS.

2. Definition of compaction efficiency

In this present research, it is assumed that the soil is completely saturated. The effectiveness of compaction can be measured by the change in the average void ratio of the specimen ($\Delta\bar{e}$), which can be calculated from the amount of water drained from the soil during the test. Since the maximum void ratio ($e_{\max}$) and the minimum void ratio ($e_{\min}$) can be measured beforehand, the compaction efficiency, η, is defined as (Wang *et al.* 2009):

$$\eta = \frac{\Delta\bar{e}}{e_{\max} - e_{\min}} \tag{1}$$

where $\bar{e}$ = average void ratio which can be calculated from.

$$\bar{e} = e_0 - \Delta e \tag{2}$$

where e_0 is the initial void ratio. It can be controlled by the test.

3. Properties of Hong Kong CDGS

The soil used in this study was excavated from a construction site at Beacon Hill, Kowloon Tong, Hong Kong. Table 1 summarizes the physical properties of this soil. It was noted that the fine content of CDGS could affect the dynamic response of the soil significantly. During dynamic compaction loading, dynamic forces disrupt the soil skeleton and force the particles to compact into a denser arrangement. As a result, the strength of the soil is improved. The properties of the fines content of CDGS in Hong Kong and the effect of fines content on the dynamic compaction grouting have been reported by Wang *et al.* (2009). In this current investigation, the fines content of the soil tested was 6%, which is shown in Table 1.

4. Schematic of experimental setup and procedures

Figure 2 shows the schematic layout of the static and dynamic compaction grouting experimental tests in a triaxial apparatus

Table 1. Physical properties of Hong Kong CDG (Wang *et al.* 2009)

Properties	Value
Natural water content	8%
Gravel	30%
Sand	64%
Fine particles (0.075 mm)	6%
D_{10}	0.18 mm
D_{30}	0.7 mm
D_{60}	1.8 mm
Coefficient of uniformity (D_{60}/D_{10})	10
Liquid limit	36%
Plastic limit	25%
Plasticity index	11%
$e_{\max}$	1.096
$e_{\min}$	0.493
Optimum moisture content	11%

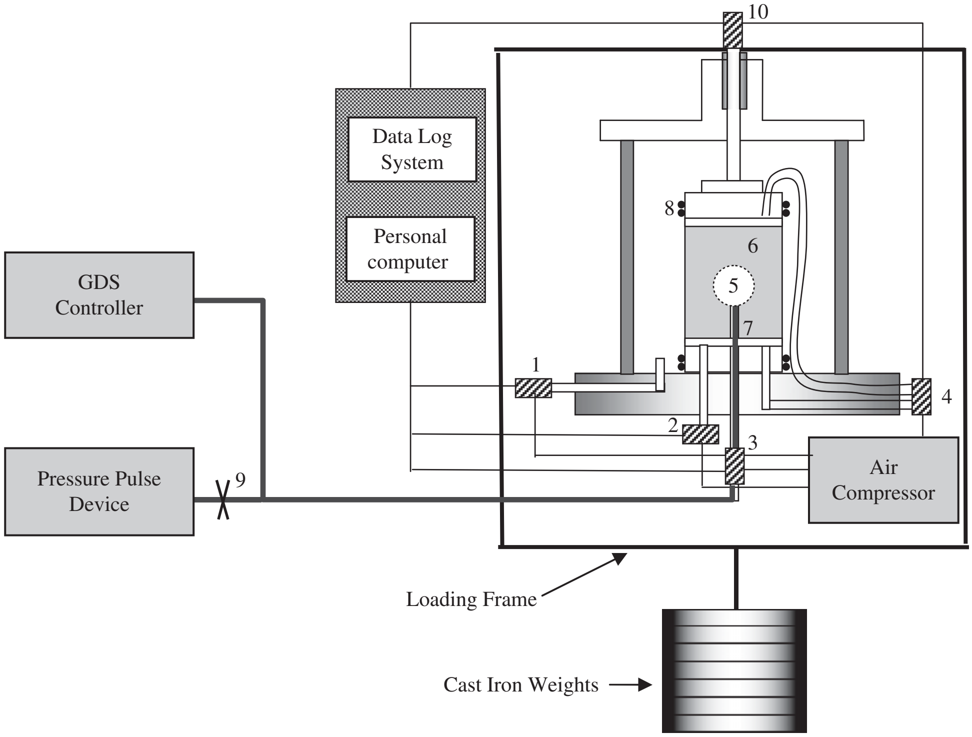

Notes:
1: Confining pressure transducer, 2: Pore water pressure transducer, 3: Injection pressure transducer, 4: Back pressure and volume change transducer, 5: Balloon, 6: Soil specimen, 7: Porous stone, 8: O ring, 9: Tap, 10: LVDT

Figure 2. Schematic layout of static and dynamic compaction grouting experimental tests (Wang *et al.* 2009).

(Wang *et al.* 2009). The diameter and height of the specimens are 75 and 150 mm, respectively. Confining pressure was applied to the specimen that was surrounded by a rubber membrane. Confining pressure was measured by transducer 1. The injection needle was located in the center of the specimen, and water could enter to expand the membrane of needle at the end of the injection tube. When the membrane was expanded by the injection water, it first needed to overcome the effect of the confining pressure applied on the soil. Further expansion would compact and densify the soil (Wang *et al.* 2010). Due to the increase of injection pressure, excess pore water pressure in the sample was generated. Pore pressure was measured by transducer 2. The injection pressure was measured using transducer 3 (see Figure 3).

Impulsive waves were produced by a wave generator. The wave motion led to the vibration of the membrane, which transmitted waves to the soil thus moving the surrounding soil particles (Wang 2006, Wang *et al.* 2009). Similarly, owing to an increase in pressure and wave propagation, excess pore water pressure was generated and would subsequently dissipate with time, which was measured by transducer 2. The amount of drained water was measured using transducer 4. During the injection process, the injection volume and the injection rate were measured by a pressure/volume controller. Vertical displacement of the specimen was measured using a linear voltage differential transformer (LVDT). In addition, the conditions for different lateral pressure coefficient (K) were obtained using a dead weight loading mechanism (Wang *et al.* 2010). All the data from the transducers were recorded automatically in a data log associated system (Wang 2006).

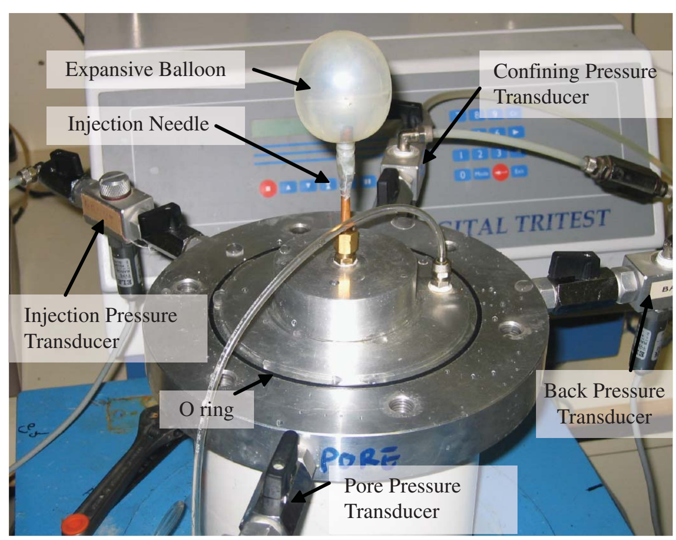

Figure 3. Modified triaxial cell base and the expanded injection needle.

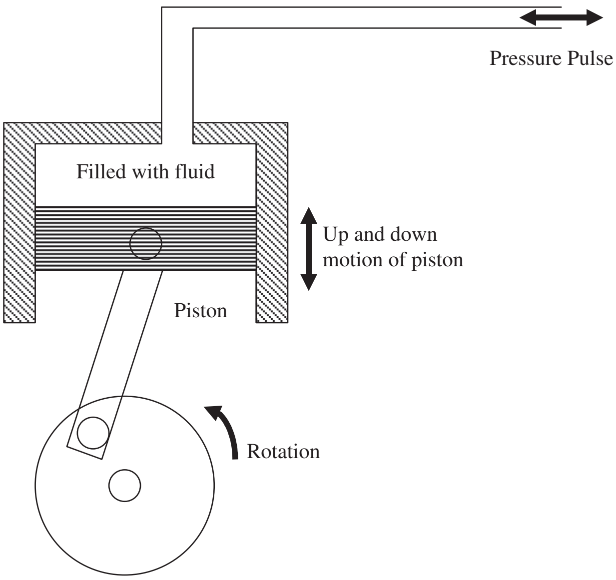

Figure 4. Schematic diagram of the Pressure Pulse Device.

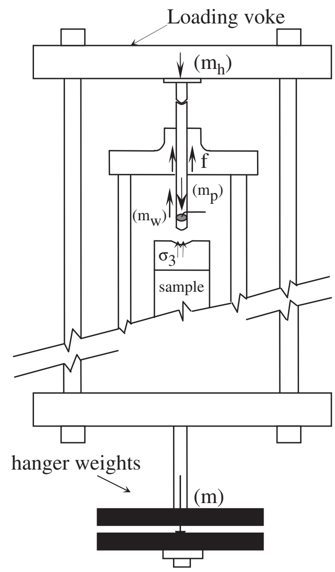

Figure 5. Anisotropic consolidation tests in triaxial cell under dead weight loading, illustrating forces acting on the specimen.

4.1 *Impulse wave generator*

Impulse wave is generated using an impulse wave generator. The impulse wave generator resembles the inside of an automobile engine. Rapid changes in pressure are generated by a piston traveling up and down inside a cylinder that is filled with the injection fluid (Wang 2006). The cylinder is connected to the grout line which transmits the pressure to the membrane. Explanation of the basic crank mechanism can be found in Richart (1970), which is shown in Figure 4.

4.2 *Loading frame for anisotropic consolidation test*

In the anisotropic consolidation test an axial load was applied to the sample during consolidation in order to maintain a constant ratio of the horizontal and vertical principal stresses (σ_h/σ_v). Figure 5 illustrates the anisotropic consolidation tests in triaxial cell with forces acting on the specimen under dead weight loading. The net downward force F applied to the sample top cap is given by (Head 1998):

$$F = \left[\frac{m_h + m + (m_p - m_w)}{1000}\right] \times 9.81 - \frac{\sigma_h a}{1000}(\mathrm{N}) \qquad (3)$$

The gravity of the top cap and piston is equal to $\frac{(m_p - m_w)\times 9.81}{1000}$ N, where m_p is the mass of top cap and piston (g) and m_w is the volume (cm^3) or mass (g) of water displaced by the top cap and the submerged part of the piston. It is assumed that the piston friction is counteracted by the effective mass of the piston and top cap ($m_p - m_w$). The axial stress σ_v is equal to $\left(\frac{F}{A} \times 1000\right) + \sigma_h$(kPa). Detailed description of the loading frame is documented by Wang (2006) and Wang *et al.* (2010). It is noted that the constant ratio of the horizontal and vertical principal stresses (σ_h/σ_v) is given in terms of total stress. Usually, the coefficient of earth pressure (K) is defined in terms of effective stresses. In the present tests, the pore pressure can be controlled at the beginning of the test.

4.3 *Sample preparation*

Soil samples for the compact grouting tests should be prepared in such a way that they are reproducible. The sample should achieve a predetermined dry density and should be homogeneous. The soil sample was prepared in the split mould in twelve layers using the moist tamping method (Ladd 1978). Every effort was made to prevent material segregation.

The wet weight of the material required was calculated for the whole sample and also for each of the twelve layers based on the dimensions of the mould and the pre-existing needle in the centre of mould. When calculating the required height of the sample at the top of the *n*th layer, it was considered that the compaction of each succeeding layer can further densify the material below it. Therefore, the concept of under-compaction (Ladd 1978) was used to make a uniform sample. The optimum percentage of under-compaction is 5% for the loose samples. The amount of material required for each layer was weighted and placed into the mould. The surface of the material can be leveled using a spatula and compacted to the predetermined height. It is important to note that the tamping rod was not touching the needle when the soil was being compacted. More detailed description of the sample preparation can be found in Wang (2006).

4.4 *Laboratory testing procedures*

The testing procedure is divided into five steps. The first step is saturation of the specimen. The second step is the consolidation of the specimen to control initial void ratio and effective confining pressure. The third step is the injection of water into the injection tube (needle) at the center of the specimen. The fourth step is applying pressure pulses to introduce vibration in the membrane and the surrounding soil (Wang *et al.* 2009). The final step is the consolidation of the soil until the back pressure and pore pressure have reached equilibrium ($\Delta u \approx 0$): i.e. consolidation has been completed. Note that the final step actually starts in the third and fourth steps in terms of the starting time of consolidation. The difference in procedures between static and dynamic compaction grouting is that dynamic compaction grouting requires the fourth step. The other steps for static and dynamic compaction groutings are the same. See Wang (2006) for more details on experimental setup.

A total of 21 static compaction grouting tests and 80 dynamic compaction grouting tests were carried out to study the static and dynamic compaction effect of the Hong Kong CDGS. Hereinto, 12 tests were carried out to study the effect of effective confining pressure on the compaction efficiency, which is summarized in Table 2. Another nine tests were performed to study the effect of injection rate on the compaction efficiency as shown in Table 3. In addition, a total of 108 dynamic compaction tests were carried out to study the effect of dynamic compaction frequency, dynamic compaction duration, the lateral pressure coefficient and initial dry density (see Table 4). Each type of test was carried out three times for repeatability and reliability of the test results. Moreover, in order to study the effect of one parameter, other parameters were kept constant during the test, i.e. static injection time was kept at 0.3 min; injection volume at 8 ml, consolidation time at 30 min, the dynamic compaction period at 1 min except for the tests to study the effect of dynamic compaction period, which the dynamic compaction period was changed.

5. Laboratory experimental results

5.1 *The effect of confining pressure on static compaction efficiency*

A series of triaxial tests were carried out with static injection of fluid into the injection needle to compact the surrounding soil inside the specimen. In these tests, the back pressure was maintained at 100 kPa, the effective confining pressure increased from 50 to 200 kPa. Since the effect of injection depth in the field can be simulated by an increase in confining pressure, the experimental results will also reflect the effect of injection depth on the compaction efficiency. Figure 6 shows the normalized void ratio e/e_0 versus time plot for different effective confining pressures. The void ratio change increases with increase in effective confining pressure from 50 to 100 kPa; however, this increase in void ratio was not significant. This is evident in the increase in compaction efficiency from 0.13 to 0.14 as shown in Figure 7. In comparison, void ratio change increases abruptly when the effective confining pressure increased up to 150 kPa, and the compaction

Table 2. Parameters to study the effect of confining pressure on compaction efficiency

Test numbers	Confining pressure	Effective confining pressure (kPa)	Radius of specimen (r) (mm)	Injection volume (V_{inj}) (cm^3)	Injection rate (q) (cm^3/min)	Initial void ratio (e_o)
3	150	50	100	8	30	0.856
3	200	100	100	8	30	0.856
3	250	150	100	8	30	0.855
3	300	200	100	8	30	0.853

Table 3. Parameters to study the effect of injection rate on static compact efficiency

Test numbers	Effective confining pressure (kPa)	Radius of specimen (r) (mm)	Injection volume (V_{inj}) (cm^3)	Injection rate (q) (cm^3/min)	Initial void ratio (e_o)
3	50	100	8	5	0.852
3	50	100	8	12	0.856
3	50	100	8	30	0.855

Table 4. Number of test in dynamic compaction grouting study

Parameter	Dynamic compaction frequency (1–18 Hz)	Dynamic compaction period (30–240 s)	Lateral pressure coefficient (0.6–1)	Initial dry density (1.3–1.4 g/cm^3)
Numbers of tests	54	24	15	15

efficiency rose to 0.27. However, when the effective confining pressure was increased to 200 kPa, there was no corresponding increase in void ratio change comparing with that of 150 kPa (Figure 6). On the contrary, void ratio change at confining pressure of 200 kPa was a little less than that of 150 kPa. Similarly, the compaction efficiency for the effective confining pressure of 200 kPa was a little less than that of 150 kPa (Figure 7). This indicates that compaction efficiency increases with an increase in effective confining pressure. However, when the effective confining pressure reaches a certain value, the grouting efficiency does not increase continuously under the same injection volume.

Figure 8 shows the injection pressure versus time for different effective confining pressures. The injection pressure increases with an increase in effective confining pressure from 50 to 200 kPa. This is due to the fact that higher injection pressure is required to expand the membrane when it is subjected to higher effective confining pressure. The injection volume is kept constant at 8 ml in each injection cycle. When the specimen is subjected to an effective confining pressure of 50 kPa, the injection pressure in the specimen decreases and become steady soon after the completion of injection. For higher effective confining pressure (100 and 200 kPa), the injection pressure decreases gradually and requires longer time to become stabilized. The higher injection pressure induces higher excess pore water pressure in the surrounding soil (Figure 9). Meanwhile, excess pore pressure dissipation will in turn influence the injection pressure until the injection pressure has reached equilibrium with the effective stress in the surrounding soil.

5.2 *The investigation of injection rate on compaction grouting*

To examine the effect of the injection rate on the compaction efficiency, two tests were performed at different injection

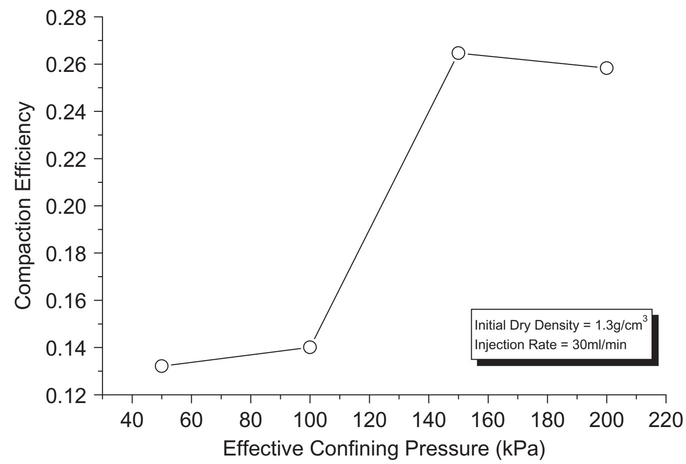

Figure 7. Compaction efficiencies versus effective confining pressure.

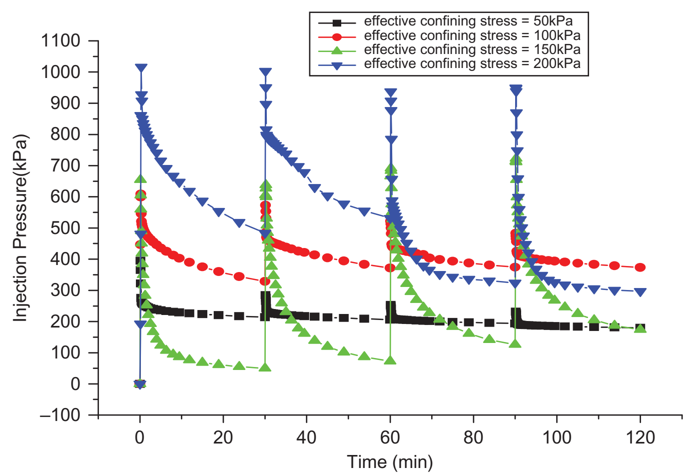

Figure 8. Injection pressures versus time for different effective confining pressure.

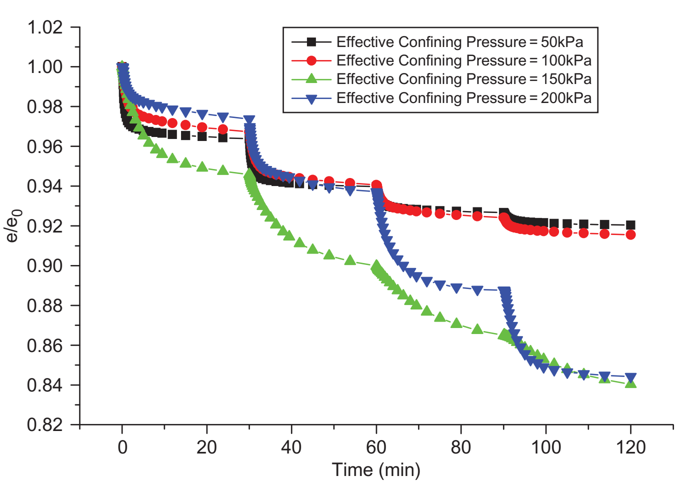

Figure 6. Normalized void ratio e/e_0 versus time for different effective confining pressure.

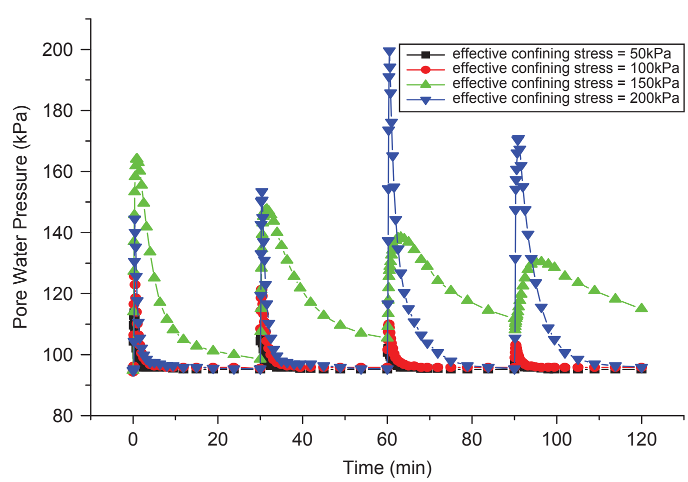

Figure 9. Excess pore water pressures versus time for different effective confining pressure.

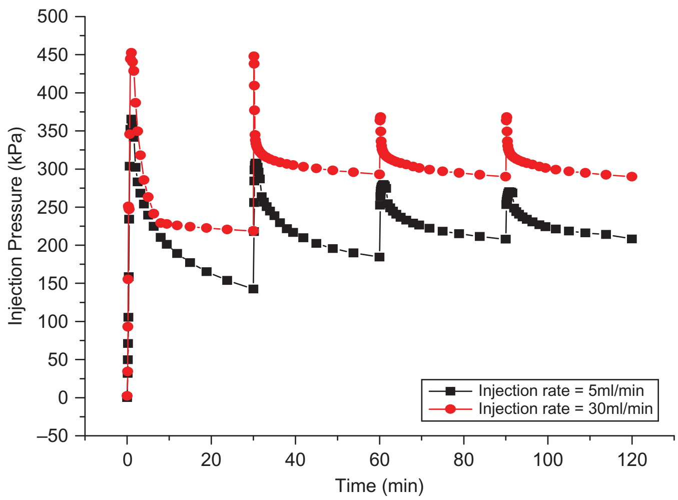

Figure 10. Injection pressure versus time for different injection rate.

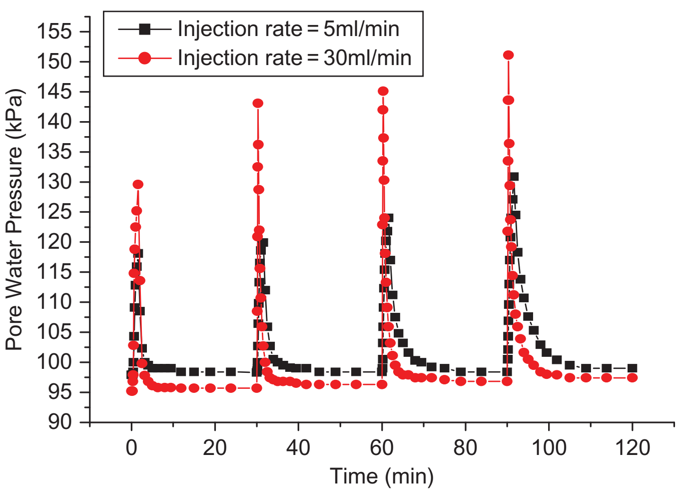

Figure 11. Pore water pressure versus time for different injection rates.

rates (5 and 30 ml/min) on the 100 mm diameter specimen. Figures 10 and 11 show the measured injection pressure and excess pore water pressure response versus time, respectively. The injection pressure and pore water pressure increases with the increase in injection rates. At slower injection rates (5 ml/min), it takes longer time to complete the injection for the same injection volume. The compaction process with slower injection rates gives a slightly lower peak pore water pressure and peak injection pressure than higher injection rate (30 ml/min). Figure 12 shows the normalized void ratio e/e_0 versus time plot for different injection rates. The void ratio change for the two tests with different injection rates are almost the same. It is because the existence of membrane of injection needle lowers the effect of injection rates to the surrounding soils, under the same injection volume.

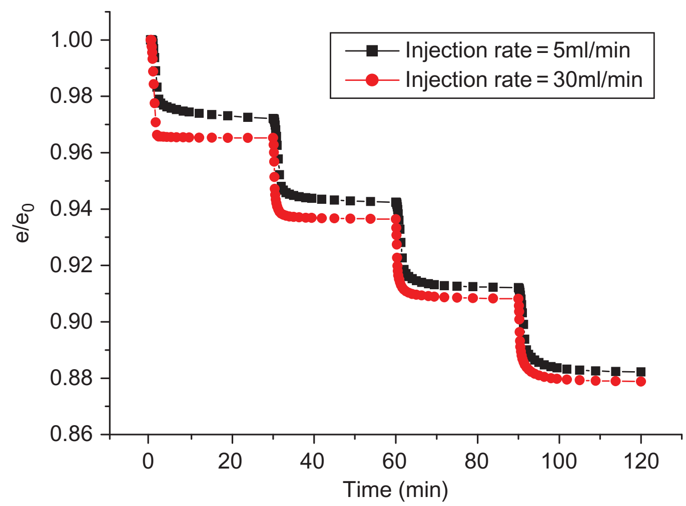

Figure 12. Normalized void ratio e/e_0 versus time for different injection rates.

5.3 *General comparison between static and dynamic compaction tests*

Figure 13 shows the normalized void ratio e/e_o versus time for static and dynamic compaction tests. The static injection time is kept constant at 0.3 min, injected volume of each cycle of 8 ml, the dynamic compaction period of 1 min, and the consolidation time of 30 min. The void ratio changes for the dynamic tests are about 3–5 times higher than the static tests (see Figure 13). Using Equation (1), the compaction efficiency for the dynamic test is 0.414. For comparison, the compaction efficiency for the static test is 0.099. Therefore, using dynamic compaction, the compaction efficiency is 4–5.5 times higher than the corresponding static tests.

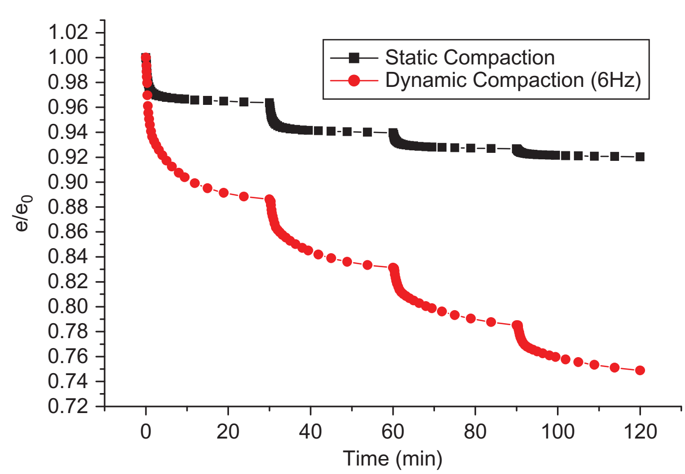

Figure 13. Normalized void ratios e/e_0 versus time for static and dynamic compaction groutings.

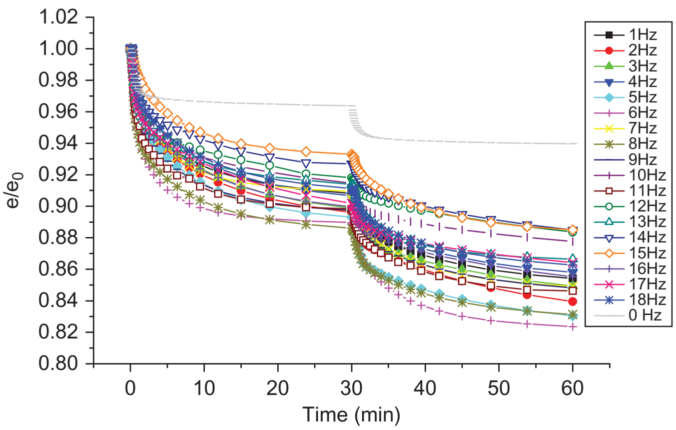

Figure 14. Normalized void ratio e/e_0 versus time for different dynamic compaction frequencies.

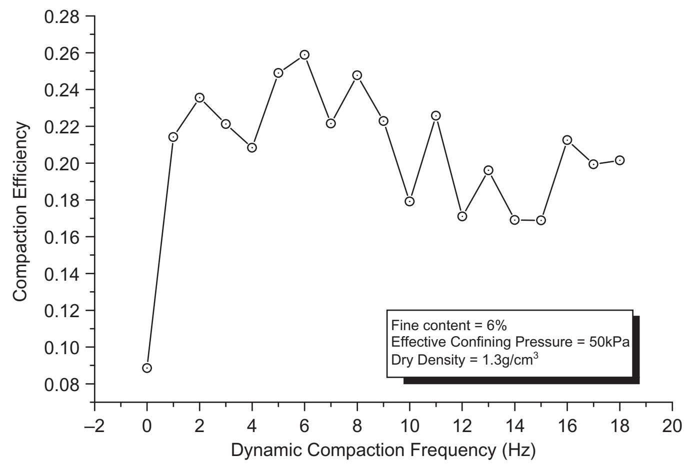

Figure 15. Compaction efficiencies versus frequency.

5.4 *Effect of dynamic compaction frequency on the compaction efficiency*

Figure 14 shows the normalized void ratio e/e_0 versus time plot for dynamic compaction frequency varying from 0 to 18 Hz. From Figure 14 the void ratio changes for all the dynamic tests are much larger than that of the static tests which are denoted by zero frequency. From Figure 15, the compaction efficiency for the dynamic compaction test is 2–3 times higher than that of the static compaction test for all cases considered. Moreover, the compaction efficiency reaches a peak value around 6 Hz and there are fluctuations of the compaction efficiency at other frequencies. For example, when the dynamic frequency is equal to 2 Hz, the compaction efficiency is a little higher than that for frequencies of 3 and 4 Hz. It is because both the dynamic amplitude and frequency may influence the compaction efficiency (Wang *et al.* 2009). Figure 16 shows the calibration of the dynamic amplitude and dynamic frequency of the pressure pulsing device. The amplitude decreases with the increase of the frequencies from 2 to 4 Hz, and becomes almost constant when the frequencies increase from 4 to 18 Hz. This is the reason for higher compaction efficiency at 2 Hz than 3 or 4 Hz because of larger amplitude. Larger amplitude can transfer more energy to compact the soil. Even though the frequencies 3 and 4 Hz are higher, the amplitudes in these cases are lower. The occurrence of peak compaction efficiency when frequency varies from 4 to 18 Hz can be related to reaching the resonance frequency of the vibrator–soil system.

The frequency of pulsing is an important parameter in dynamic soil compaction. During the compaction phase, the objective is transferring energy to the surrounding soil as efficiently as possible. It is best achieved if the membrane of the injection needle is vibrating at or close to the resonant frequency of the soil. In this case, the optimum frequency is about 6 Hz. Resonant frequency depends on several factors, such as the mass of the vibrating device, the size of the membrane, density of soil, boundary conditions and the wave velocities of the soil. The resonant frequency will increase with increasing

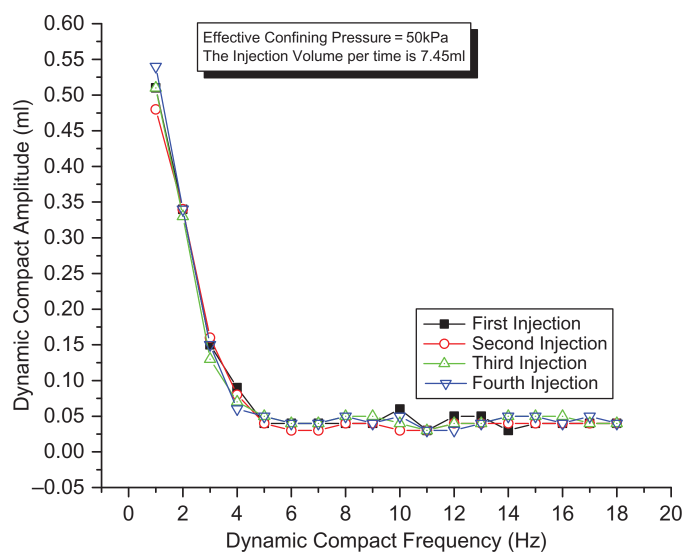

Figure 16. Dynamic compaction amplitudes versus frequency.

shear wave velocity, reflecting a change in soil stiffness and soil strength (Massarsch and Westerberg 1995).

The relative density D_r of a soil is an important measure to evaluate the degree of soil improvement (Wang *et al.* 2009). Figure 17 shows the relative density versus dynamic frequency. For example, when the dynamic frequency is 6 Hz, the initial relative density for the soils is about 0.4, as a comparison, the relative density increases to around 0.7 after dynamic compaction. It indicates that the soil is densified from a soft or loose state to a densified state. In addition, for the frequency of 0 (static compaction), the initial relative density is equal 0.4, and the final relative density is only 0.5 after compaction, while the maximum D_r is 1. It means that the soil could be further densified. In contrast, For the frequency of 6, the initial relative density is also 0.4, but the final relative density after compaction is about 0.7, which means that there is less room for improvement. From this comparison, it also proves that the

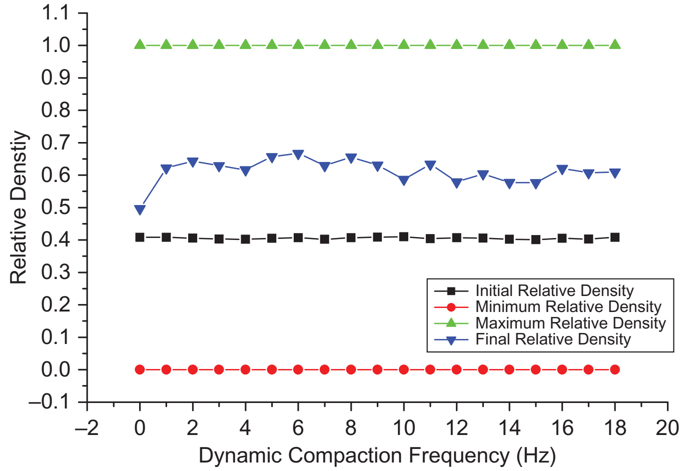

Figure 17. Relative densities versus dynamic frequency.

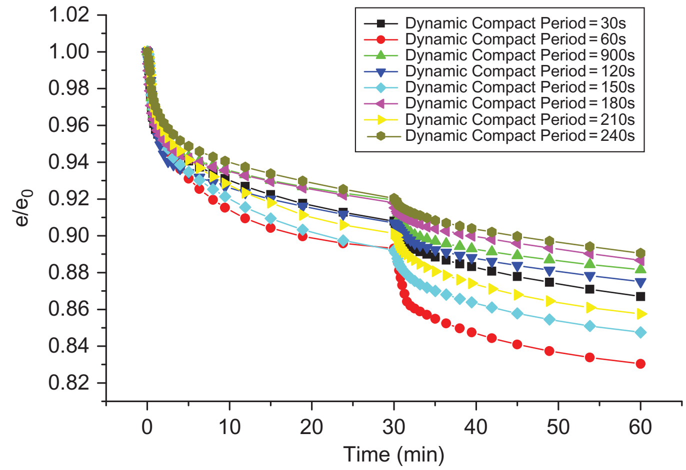

Figure 18. Normalized void ratio e/e_0 versus dynamic compaction period (Time is the whole time from the first injection to the end of second consolidation).

method of dynamic compaction is much more efficient than that of static compaction in soil improvement.

5.5 *Effect of dynamic compaction period on compaction efficiency*

The normalized void ratio e/e_0 versus time plot for different dynamic compaction periods are shown in Figure 18. The dynamic compaction period is the duration of applying the pressure pulse to the surrounding soil. In order to compare the effect of the compaction period on the compaction efficiency, the frequency is kept constant at 6 Hz. Optimum compaction efficiency occurs at a period of 60 s as shown in Figure 19. It indicates that longer compaction period does not in general give higher compaction efficiency. Therefore, identifying an optimum dynamic compaction period is necessary in order to provide effective compaction and reduce the cost of soil improvement. Certainly, an optimum dynamic compaction period depends on many factors such as the dynamic frequency, amplitude, the properties of soils and the boundary conditions. The void ratio change is not directly proportional to the compaction period (see Figure 18).

5.6 *Effect of lateral pressure coefficient k on the compaction efficiency*

The initial lateral earth pressure coefficient (K) has an effect on soil behavior. A K value of 1 means isotropic stress state. Figure 20 shows that the void ratio changes due to dynamic compaction are strongly affected by the lateral pressure coefficient. The higher the lateral pressure coefficient, the lower the void ratio changes. The compaction efficiency decreases from 0.29 to 0.216 when the lateral pressure coefficient increases from 0.6 to 1.0 (see Figure 21). In particular when the lateral pressure coefficient increases from 0.6 to 0.7, the compaction efficiency shows an evident decrease.

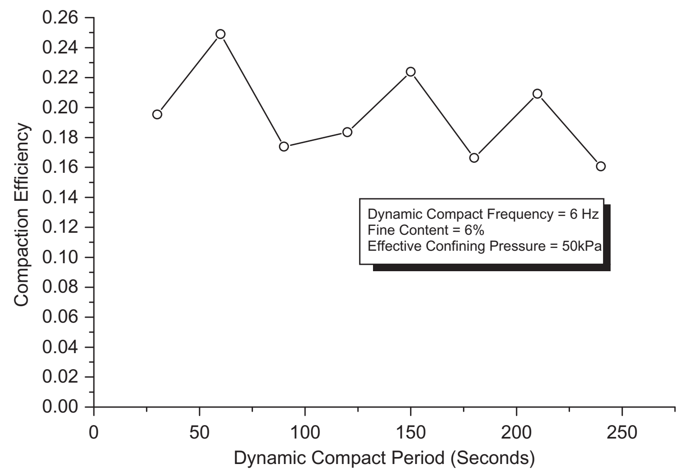

Figure 19. Compaction efficiencies versus dynamic compaction period.

5.7 *Effect of initial dry density on the compaction efficiency*

Figure 22 shows the normalized void ratio e/e_0 versus time for different initial dry densities. The void ratio change decreases with increasing initial dry density. Similarly, the compaction efficiency decreases with increasing initial dry density (see Figure 23). For example, the compaction efficiency is 0.21 when the initial dry density is 1.3 g/cm^3, while the compaction efficiency decreases to 0.17 when the initial dry density is 1.7 g/cm^3. It is because the softer/looser the soil, the easier the soil to be compacted.

6. Potential practical applications of the test results

The results of this study can be used to develop a better understanding of the fundamental behavior of dynamic compaction grouting in CDGS of Hong Kong. The compaction efficiency

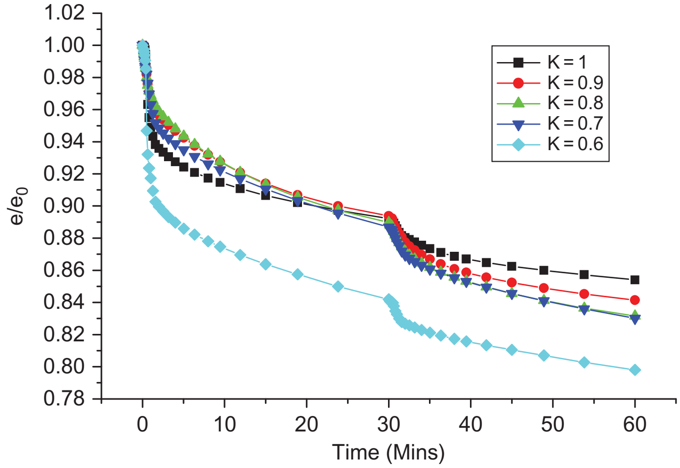

Figure 20. Normalized void ratio e/e_0 versus time for different lateral pressure coefficient (*K*) (Time is the whole time from the first injection to the end of second consolidation).

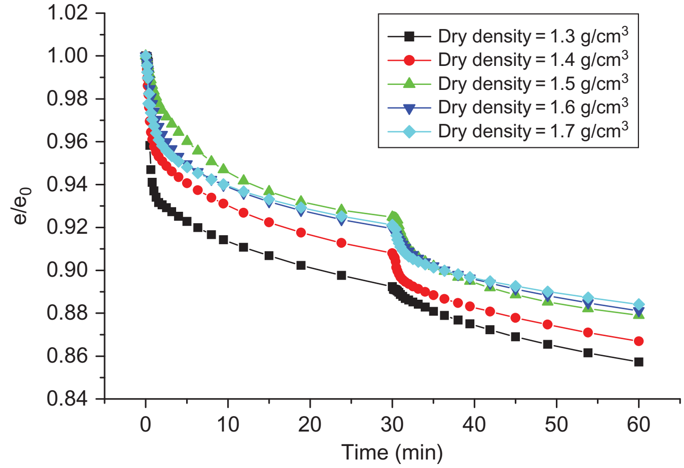

Figure 22. Normalized void ratio e/e_0 versus time for different dry density.

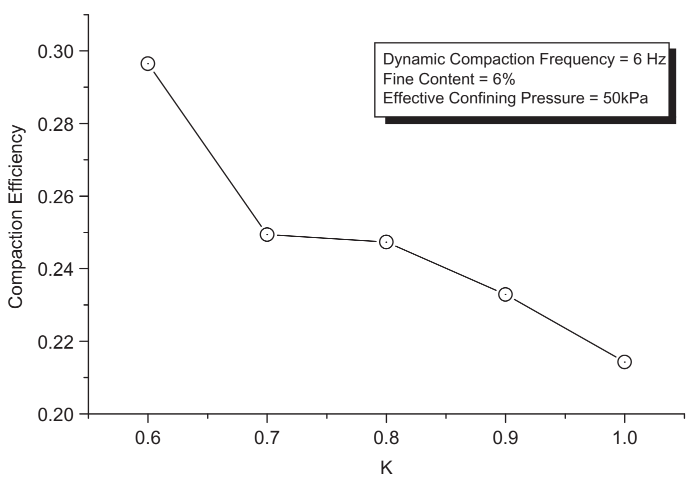

Figure 21. Grouting efficiency versus lateral pressure coefficient (*K*).

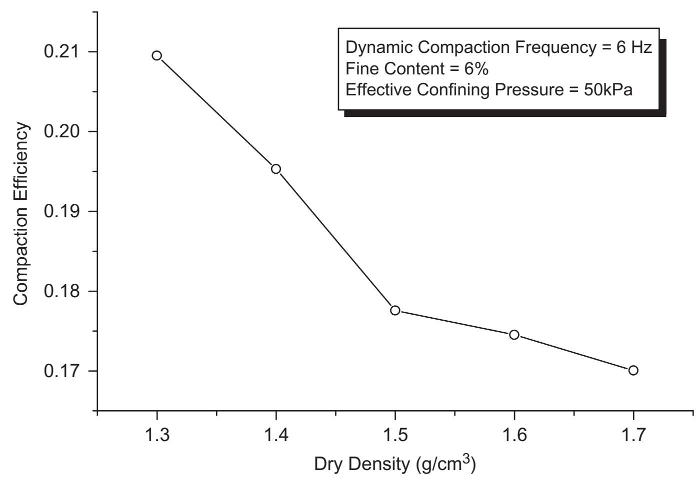

Figure 23. Compaction efficiencies versus time for different dry density.

varies as a function of dynamic compaction frequency and period. It depends on the soil properties prior to compaction, the required degree of densification, and the vibration energy transferred to the ground. Moreover, these parameters may be affected by conditions of the outer boundary, such as the lateral pressure coefficient and the effective confining pressure. It is noted that the grout is kept separated by the membrane from the surrounding soil, which means that the composition of the surrounding soil does not change during this process. In practical applications, the membrane can be replaced by a geotextile bag. Naudts and van Impe (2000) used to adopt this technique by installing a geotextile bag around the sleeves of the injection pipes during the process of compaction grouting. The expansion of the membrane (geotextile bag) can fill the spaces that are lost due to the decrease in volume of the soil as a result of the densification process. This prevents the loss of ground due to the densification process. Other vibrational techniques such as vibro-compaction or vibro-flotation require filling of the ground due to the compaction process. This loss of ground can result in settlement during the densification process and cause damages to nearby structures and utilities.

Usually traditional static compaction grouting is used to generate upward displacement of the ground surface to compensate the settlement induced by tunneling or excavation. However, in some cases, for the static compaction grouting, only the shear strength enhancement of soil is desired, while heaving of the ground surface is not necessary or even deleterious. The shear strength enhancement is actually related with the reduction of void ratio in this paper. Although the injection volume can lead to the expansion of soil (be responsible for heaving of the ground), the shear strength enhancement is based on the consolidation of the soil that results in the soil contractive (be responsible for the settlement of ground). Therefore, if the grouting parameters, such as injection volume and injection pressure of static compaction grouting, dynamic compaction frequency and period of dynamic compaction grouting can be controlled, a balance between the displacement of ground surface and the shear strength enhancement can be reached. Furthermore, in practical application, considering the higher efficiency of dynamic compaction grouting (three times higher than that of static compaction grouting), the static and dynamic compaction can be performed at the same time, i.e. the static compaction grouting is performed first, followed by the dynamic compaction grouting.

7. Conclusions

To study the mechanism of static and dynamic compaction grouting in CDGS of Hong Kong, a triaxial apparatus was modified and presented. A pressure pulse device is invented to introduce pulse waves into the soil during the compaction process. Compaction efficiency is defined as a measure of the effectiveness of the compaction in soils. Laboratory experimental results show that CDGS compacted using the dynamic compaction method has compaction efficiency 2–5 times higher than the static method. The results depend on different dynamic compaction frequency, amplitude and period. The results give a better understanding of the fundamental behavior of the static and dynamic compactor grouting in CDG soils.

Acknowledgements

Financial support for this project was partly provided from the RGC grants (Project No. 9040593 and CityU 1178/03E) of the Government of Hong Kong. The generous support in providing equipment needed for experimental portion of this research from the University of Hong Kong is gratefully acknowledged.

References

Au, S.K.A., 2001. Fundamental study of compensation grouting in clay. PhD thesis, University of Cambridge, Cambridge, UK.

Au, S.K.A., Yeung, A.T., Soga, K. and Cheng, Y.M., 2007. Effects of subsurface cavity expansion in clays. *Geotechnique* 57 (10), 821–830.

Baker, W.H., Cording, E.J. and MacPherson, H.H., 1983. Compaction grouting to control ground movements during tunneling. *Underground Space*, 7, 205–212.

Baker, W.H., 1985. Embankment foundation densification by compaction grouting, *Proceedings, Issues in dam grouting*, ASCE, New York, pp. 104–122.

Boulanger, R.W. and Hayden, R.F., 1995. Aspects of compaction grouting of liquefiable soil. *Journal of Geotechnical Engineering*, 121 (12), 844–855.

Charles, J.A. and Watts, K.S., 2002. *Treated ground engineering properties and performance*. CIRIA C572, London.

Graf, E.D., 1969. Compaction grouting technique. *Journal of Soil Mechanics and Foundation, Division, ASCE*, 95 (5), 1151–1158.

Graf, E.D., 1992. Compaction grout. In Grouting, soil improvement and geosynthetics. ASCE *Geotechnical Special Publication*, Reston, VA: American Society of Civil Engineers, Vol. 1, No. 30, pp. 275–287.

Greenwood, D.A. and Kirsch, K., 1984. Specialist ground treatment by vibratory and dynamic methods, in *Advances in piling and ground treatment*, *Proceeding of International Conference*, London: Thomas Telford, pp. 17–45.

Head, K.H., 1998. *Manual of soil laboratory testing*. Vol. 3. Chichester, UK: John Wiley.

Jebe, W. and Bartels, K., 1983. The development of compaction methods with vibrators from 1976 to 1982, in *Proceedings of 8th Europe Conference of Soil Mechanics and Foundation Engineering*, Helsinki, 1983 Rotterdam: AA Balkema, Vol. 1, pp. 259–266.

Ladd, R.S., 1978. Preparing test specimens using undercompaction. *Geotechnical Testing Journal*, 1 (1), pp. 16–23.

Mair, R.J., Harris, D.I., Love, J.P., Blakey, D. and Kettle, C., 1994. Compensation grouting to limit settlement during tunneling at Waterloo station, London, in *Tunnelling '94*, Institution of Mining and Metallurgy, London: Chapman and Hall, pp. 279–300.

Massarsch, K.R. and Westerberg, E., 1995. The active design concept applied to soil compaction, in *Proceedingss of the Bengt B. Broms Symposium in Geotechnical Engineering*, Singapore, 13–15 December, pp. 262–276.

Mitchell, J.M. and Jardine, F.M., 2002. *A guide to ground treatment*. London: CIRIA C573,.

Naudts. A. and van Impe, R., 2000. An alternate compaction grouting technique, in *Proceedings of the Geodenver 2000 Conference Advances in Grouting and Ground Modification*, Denver Geotechnical Special Publication, Vol. 104, pp. 32–41.

Richart, F.E., 1970. *Vibrations of soil and foundations*. Englewood Cliffs, NJ: Prentice-Hall.

Slocombe, B.C., Bell A.L. and Baez J.I., 2000. The densification of granular soils using vibro methods. *Geotechnique*, 50 (6), 715–725.

Soga, K., Au, S.K.A., Jafari, M.R. and Bolton, M.D., 2004. Laboratory investigation of multiple grout injections into clay. *Geotechnique*, 54 (2), 81–90.

Wang, S.Y., 2006. Fundamental study of static and dynamic compaction grouting in completely decomposed granite, PhD Dissertation. City University of Hong Kong, Hong Kong, PR China.

Wang, S.Y., Chan, D. and Lam, K.C., 2009. Experimental study of the effect of fines content on dynamic compaction grouting in completely decomposed granite of Hong Kong. *Construction and Building Materials*, 23 (3), 1249–1264.

Wang, S.Y., Chan, D. and Lam, K.C., 2010. Effect of lateral earth pressure coefficient on pressure controlled compaction grouting in triaxial condition. *Soils and Foundations*, 50 (3), 441–445.

Warner, J., and Brown, D.R., 1974. Planning and performing compaction grouting. *Journal of the Soil Mechanics and Foundations Division, ASCE*, 100 (GT6), Proc. Paper 10606, pp. 653–666.

Warner, J., 1992. Compaction grout; rheology vs. effectiveness, in *Grouting, soil improvement and geosynthetics*. ASCE Geotechnical Special Publication. Vol. 1, No. 30. Reston, VA: American Society of Civil Engineers, pp. 229–239.

Younis, M.A., 1994. Small scale physical modeling of compaction grouting, Masters Thesis Presented to the University of Maryland at College Park.